# WATER QUALITY IMAGE CLASSIFICATION FOR AQUACULTURE USING DEEP TRANSFER LEARNING

*H. Guo*[*], *X. Tao*[†], *X. Li*[‡]

**Abstract:** With the development of high-density and intensive aquaculture production and the increasing frequency of water quality changes in aquaculture water bodies, the number of pollution sources in aquaculture ponds is also increasing. As the water quality of aquaculture ponds is a crucial factor affecting the production and quality of pond aquaculture products, water quality assessment and management are more important than in the past. Water quality analysis is a crucial way to evaluate the water quality of fish farming water bodies. Traditional water quality analysis is usually obtained by practitioners through experience and visual observation. There is an observability deviation caused by subjectivity. Deep transfer learning-based water quality monitoring system is easier to deploy and can avoid unnecessary duplication of efforts to save costs for aquaculture industry. This paper uses the transfer learning model of artificial intelligence to analyze the water color image automatically. 5203 water quality images are collected to create a water quality image dataset, which contains five classes based on water color. Based on the dataset, a deep transfer learning-based classification model is proposed to identify water quality images. The experimental results show that the deep learning model based on transfer learning achieves 99 % accuracy and has excellent performance.

Key words: *aquaculture, water quality, transfer learning, deep learning*

*Received: June 26, 2020* **DOI:** 10.14311/NNW.2023.33.001
*Revised and accepted: February 28, 2023*

## 1. Introduction

Aquaculture is the fastest-growing sector of global food production. This "Blue Revolution" produced more fish for human consumption than global fisheries for the first time in 2014. Continuing this growth in aquaculture, a relatively energy-efficient form of food production, is necessary to meet global food demand, for which

[*]Hao Guo; School of Software and Blockchain, Jiangxi Institute of Applied Science and Technology, 330100, Nanchang, China
[†]Xunlin Tao; College of International Business, Jiangxi Institute of Applied Science and Technology, 330100, Nanchang, China
[‡]Xingcun Li – Corresponding author; School of Management, Huazhong University of Science and Technology, 430074, Wuhan, China, E-mail: lixingcun97@gmail.com

a 50 % increase will be needed globally by 2050 with higher increases required in lower-income and middle-income countries [4]. Similar to traditional agriculture, the continuous growth and long-term sustainability of aquaculture have high standards for the quality of aquaculture water bodies. With aquaculture occurring in ponds, reservoirs, and lakes of urban and peri-urban environments, many operations are already knowingly or unknowingly using "non-traditional" (or raw sewage or treated sewage effluent) waters [4]. The sustainable environmental quality of developed countries [29] and developing countries [10] has attracted researchers' attention. Issues related to water quality in aquaculture are discussed in these papers.

In aquaculture, water quality issues cannot be ignored. The quality of water directly affects the growth and development of aquaculture objects, and any aquaculture animal needs a water quality condition suitable for its survival. If the water quality can meet the requirements of aquaculture, aquaculture animals can grow well. If some metrics of water quality are beyond the range of biological adaptation and tolerance, aquaculture organisms cannot grow normally [1]. Serious water quality problems are likely to cause large-scale deaths of aquaculture animals and cause significant economic losses. There are many examples of losses caused by the deterioration of water quality during the breeding process. According to statistics, 85 % of aquatic diseases are directly caused by the deterioration of water quality. Besides, dissolved oxygen in water is an important factor that affects the aquatic animal's food intake and food digestion, and absorption rate, as well as the growth rate and feed factor [11, 28]. The quality of water directly affects the economic benefits of aquaculture. Therefore, the analysis and management of aquaculture water quality have important research value.

The quality of aquaculture water is generally analyzed from the following two aspects. On the one hand, conventional water quality tests are used to measure whether the various metrics of the water body are suitable for the growth of aquaculture animals [17, 18, 25, 26]. On the other hand, in the actual process, the water quality of the aquaculture water body is usually observed by aquaculture practitioners with practical experience to analyze the water quality.

Water quality tests are based on various physical and chemical metrics that affect water quality so that water quality can be adjusted to the best state through real-time detection. The physical and chemical metrics to be understood in aquaculture are transparency, dissolved oxygen, pH, hydrogen sulfide, nitrite, ammonia nitrogen, and heavy metals [24, 31].

However, it is difficult to assess through the traditional monitoring of the water quality in short periods, which is essential for planning, evaluation, and health management of water bodies [30]. In practice, experienced aquaculture personnel can judge water quality by observing the color of the water. This phenomenon is due to after injecting water into the fish pond, the color of the water will change due to the presence of dissolved substances, suspended particles, and plankton in the water. The expression of water color is mainly related to the type and quantity of plankton. When the types and numbers of plankton are different, the water of the pond will show different colors due to the differences in pigment cells in different phytoplankton. The duration of water color maintenance is determined by the survival time of plankton and the alternation of generations. Different water quality conditions will show different water colors.

Although experienced fishery practitioners can regulate water quality by observing changes in water quality to maintain the dynamic balance of phytoplankton, microorganisms, and zooplankton in the aquaculture ecosystem, these judgments are obtained through experience and visual observation. There are observational deviations caused by subjectivity, which reduces the comparability and repeatability of the observation results, resulting in weak generalizability of this method.

Deep learning is a significant breakthrough in the field of artificial intelligence in the past decade. The concept of deep learning originates from the study of artificial neural networks. Deep learning combines low-level features to form more abstract high-level representation attribute categories or features to discover distributed feature representations of data. The motivation for studying deep learning is to build a neural network that simulates the human brain for analysis and learning. By imitating the mechanism of the human brain's interpretation of data, deep learning has been widely studied and applied in image recognition, natural language processing, and text sentiment analysis [8, 15, 32].

In many research areas, the collection of image datasets is relatively tricky, and there is a lack of reliable experts to label the images. Transfer learning is proposed. In the field of computer vision, transfer learning is usually based on the use of pre-trained models for fine-tuning, or training with pre-training weights as initialization options. A pre-trained model is a model trained on a large benchmark dataset (such as ImageNet) to solve similar problems. Such pre-trained models usually have excellent image feature extraction capabilities. Therefore, based on pre-trained models on the large-scale dataset, researchers can fine-tune deep learning models for problems and needs in different fields [23].

Although the classification of river water quality image has received the attention and thought of researchers [12, 16, 21]. However, water quality issues remain challenging in the aquaculture industry. Aquaculture personnel analyzes aquaculture water quality by observing water color. This method has accumulated much experience and has been successful. Although this method is active, it is often based on personal experience and is difficult to generalize. How to translate these experiences into scientific, quantifiable digital information, in the modernization and creative process of aquaculture, this problem is needed to be solved urgently. The main contributions of this paper are as follows:

1. 5203 images of aquaculture water quality are collected to create a water quality image dataset, which is divided into 5 classes according to water color.

2. This is the first paper that uses deep transfer learning to solve automatic water quality image classification in aquaculture and complete water quality analysis.

3. In the experiments, the performance of the proposed model is evaluated. The experimental results show that the proposed model achieves an accuracy of 99 % and is promising for practical applications.

The remaining sections are organized as follows. Section 2 presents the dataset, methodology, and model details. Section 3 explains the experimental setup, and shows and analyzes the performance evaluation results. The conclusion is obtained in Section 4.

# 2. Materials and methods

## 2.1 Dataset

Excellent water quality usually has the following characteristics: The water color is fresh and lively, which changes with the change of light and time, which is a manifestation of the vigorous reproduction of phytoplankton. The water is fresh and tender, and there is much digestible phytoplankton. The water surface is refreshing, with no floating membrane, good transparency, and high dissolved oxygen content. The color of poor water is clear, and the transparency is too high, usually above 60 cm. Filamentous algae and aquatic vascular plants grow in water.

The color of water quality is categorically divided into the following types: (1) Dark green. The water surface often has a dark green or yellow-green floating membrane, and there are many Volvocales and euglena. (2) Gray-blue: Low transparency, high turbidity, and more cyanobacteria such as Oscillatoria in water. (3) Blue-green: Low transparency, high turbidity, gray-yellow-green floating membrane on the water surface in hot weather, and more blue-green such as Microcystis and Cystococcus in water. (4) Brown (including yellowish-brown, reddish-brown), mostly diatoms, and sometimes Cryptomanas reproduces in brown, and there are more Chlorella and Scenedesmus. (5) Green (including oil green, yellow-green, and brownish-green): The dominant species are mostly green algae (such as Cladophora, Aegagropila, and Scenedesmus) and Cryptomanas, sometimes with more Diatoms [2,6,19].

As for data acquisition, a total of 5203 water quality images are collected in a real aquaculture environment using unified digital cameras, and these images are classified into 5 classes according to water color criteria. The resolution of all images in the dataset is resized to $224 \times 224$. Details of the water quality image dataset are shown in Tab. I.

| Label | Water color | Number of images |
|---|---|---|
| 0 | dark green, light green | 1051 |
| 1 | gray blue | 1044 |
| 2 | blue-green | 1078 |
| 3 | yellowish brown, reddish brown, | 1024 |
| 4 | oil green, yellow green, brownish green | 1006 |

**Tab. I** *Details of the water quality image dataset.*

The label in Tab. I is the correct classification label for this type of image in the dataset. There are five categories in total, ranging from 0–4. A larger label value corresponds to better water quality. The water color indicates all the water colors contained in this label. The number of images per label is shown in the third column of Tab. I.

The primary purpose of image preprocessing is to eliminate irrelevant information in the image, restore real useful information, enhance the detectability of the relevant information and simplify the data to the greatest extent, thereby improving the reliability of feature extraction and image classification. The contribution of normalization also includes the ability to confine the preprocessed data to a certain range (e.g., $[0,1]$ or $[-1,1]$), thus eliminating the undesirable effects caused by odd sample data. Because the softmax activation function is used for final classification, the labels in the dataset need to be one-hot encoding. To prevent the gradient of some activation functions from being too small and accelerate convergence, the input of the network model needs to be normalized. It can be calculated by the following formula:

$$x_{\text{nor}} = \frac{x_{\text{ori}}}{255}, \tag{1}$$

where $x_{\text{ori}}$ represents the original input, $x_{\text{nor}}$ represents the normalized data, and they all belong to the float type.

## 2.2 Transfer learning

Deep learning has made significant breakthroughs in a series of fields such as image recognition and natural language processing. Convolutional neural networks in deep learning were initially proposed to solve the problem of image recognition. At present, the applications of deep learning in image recognition are mainly concentrated in the fields of image classification, object detection, and image segmentation.

There is an interesting linear positive correlation between the amount of training data required for deep learning models and the model size. Once the model is large enough, the connections between different parts of the data can be better captured by the model (such as textures and shapes in the image) and the details of the problem to be solved (such as the number of classifications). The lower layers of the model are usually used to learn the potential connections of input data (such as image edges and subjects). The back-end level of the model is usually used to learn the combination of features that are beneficial to make the final decision. It is usually used to distinguish the detailed information of the target output. Therefore, the higher the complexity of the problem to be solved (such as image classification), the higher the number of parameters and the amount of training data required. In Fig. 1, each model usually has tens of millions of parameters to participate in image feature extraction and classification decisions.

In most cases, facing a specific problem in a particular field, it is not easy to find sufficient training data. It is a common problem in deep learning applications. However, thanks to the help of technology, models trained from other data sources can be reused in similar fields after certain modifications and improvements, which significantly alleviates problems caused by insufficient data sources, and this key technology is transfer learning.

Transfer learning in computer vision usually trains deep learning models on datasets with a large number of images and categories, such as ImageNet. After training on large-scale datasets such as ImageNet, the image recognition and reusability of transfer learning models are strong. Because after much learning of the model, the model's feature extraction capability for the image has been improved, such as edge detection and curve detection. Pre-trained weights can be used as the initial weights of the model and transfer learning can be performed on datasets from various domains. Transfer learning can also be performed by freezing some modules of the pre-trained model and fine-tuning the remaining modules. Because the pre-trained model has previously learned the organizational data patterns, this smaller-scale network only needs to learn the specific connections in the data for specific problems. The Top-1 accuracy of the classic transfer learning model in ImageNet is shown in Fig. 1.

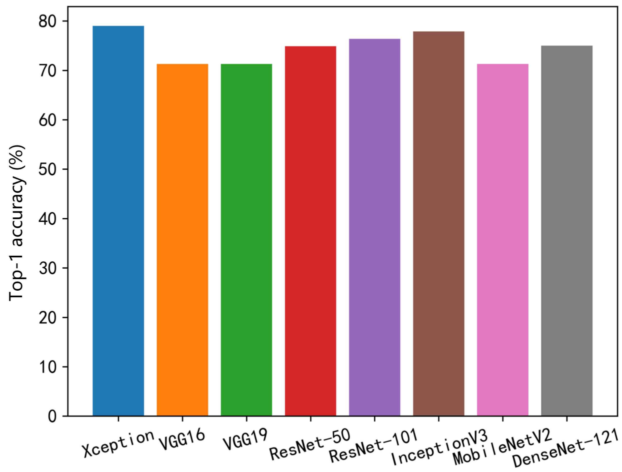


**Fig. 1** *The Top-1 accuracy of the classic transfer learning model in ImageNet.*

From Fig. 1, it can be found that the Top-1 accuracy of Xception and InceptionV3 in ImageNet is relatively high, close to 80 %. In Fig. 1, each Top-1 accuracy refers to the correct rate of the final result by taking the category with the highest probability among the category probability vectors predicted by the model.

It is worth mentioning that the advantages brought by transfer learning are not limited to reducing the size of the training data, but can also effectively avoid overfitting, that is, the modeling data exceeds the fundamental category of the problem to be solved. Once the training data is used, testing the system with other samples may cause unexpected errors. However, because transfer learning allows the model to learn from different types of data, its performance in capturing the internal connections of the problem to be solved is even better.

## 2.3 Proposed method

Although transfer learning can significantly reduce the amount of training data required by the model, it also means more professional tuning. Obtaining a dataset of an appropriate size and selecting a suitable pre-trained model are two common problems in the application of transfer learning. The amount of data in the dataset in this paper compares the amount of data in transfer learning with other applications, and a suitable amount of data is selected. Therefore, the dataset in this paper is sufficient to complete the learning of the transfer learning model. According to Fig. 1, the performance of Xception is excellent in these typical transfer learning models. This paper proposes a transfer learning model based on Xception. This model is used to learn from the water quality dataset to complete water color image classification based on water color.

### 2.3.1 Feasibility study of transfer learning in water quality image recognition

As shown in Fig. 2, in transfer learning, researchers aim to use the knowledge learned from the source task to help the model to learn how to solve another target task. For example, a pre-trained image classification network model can be used for another task related to image recognition. The water color analysis problem of the water quality image dataset and the classification problem of the ImageNet image dataset are both image recognition tasks. Therefore, the pre-trained model trained on ImageNet has good adaptability to complete the water color analysis.

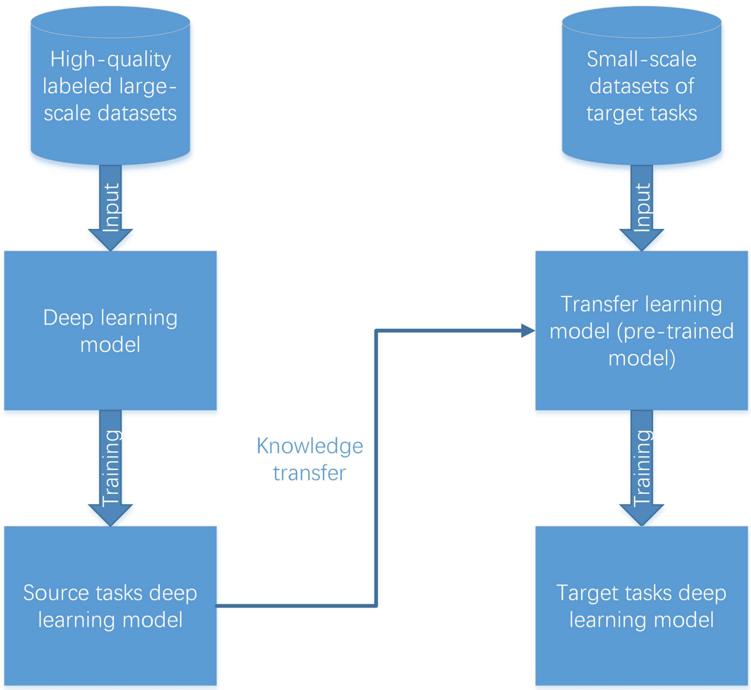


**Fig. 2** *The mechanism of transfer learning in deep learning.*

### 2.3.2 Xception

Xception assumes that spatial convolution and deep convolution are irrelevant, so it is better to operate these two steps separately. In the InceptionV3 module, the correlation and spatial correlation between channels are still not completely separated, because the $3 \times 3$ or $5 \times 5$ convolution kernel is still multi-channel input. Therefore, Xception first performs spatial convolution on a depth-by-depth basis and then performs depth convolution by $1 \times 1$ convolution to decouple spatial convolution and depth convolution. The results show that the number of Xception parameters is similar to InceptionV3, but the final effect of Xception is better than InceptionV3. In addition to replacing the InceptionV3 module with a deep separable convolution, Xception was also inspired by ResNet and added a residual design. Xception consists of 36 convolutional layers, which can be divided into 14 modules. In addition to the first and last modules, there are residual designs between the remaining modules. The difference between the deep separable convolution and the InceptionV3 module is: (1) The order of the convolution is different. The deep separable convolution is first spatially convolutional, and then $1 \times 1$ convolution. InceptionV3 module first $1 \times 1$ convolution and then spatial convolution. (2) The ReLU function is not activated between the two convolutions of the deep separable convolution, because non-linear activation may cause loss of important information. The two convolutional layers in the InceptionV3 module are processed by a non-linear activation function [5].

### 2.3.3 Proposed model

Because Xception performs prominently in the classic transfer learning model, and Xception has relatively few parameters and belongs to a lightweight network. Therefore, Xception is used as the primary model architecture for the proposed model. Nevertheless, Xception needs some modifications to adapt to the water quality image classification problem. The modification process of Xception is divided into three parts. In the first part, the no-top Xception pre-trained model is selected as the basic model of the proposed model to complete the feature extraction function of the image. No-top refers to the last fully connected layer of the model Xception being removed. In the second part, after the basic model of Xception is added, a fully connected layer of 1024 units is added to filter the extracted image features. In the third part, a five-unit fully connected layer is used as the output layer to complete the probabilistic output of water quality image classification. Between these fully connected layers, dropout with a probability of 0.4 and batch-normalization layers are added to prevent overfitting. These two fully connected layers are able to automatically filter discriminative features from the feature vector obtained by the feature extractor. The weight of no-top Xception trained in ImageNet is used as the initialization weight of the basic model for the proposed model. The remaining two fully connected layers are initialized randomly.

Since the size of the dataset is sufficient for transfer learning, the possibility of overfitting is well controlled. Therefore, all layers of the network model are not frozen, and the entire model is trained to complete the learning of the proposed model. Besides, because the datasets are similar, the features detected by the original network layer can be used for new datasets. Therefore, the original weight on the network layer can be used as the initial value. The training speed is improved due to the initialization weights that already contain favorable convolutional kernel parameters from the ImageNet dataset. The main structure of the proposed model is shown in Fig. 3.

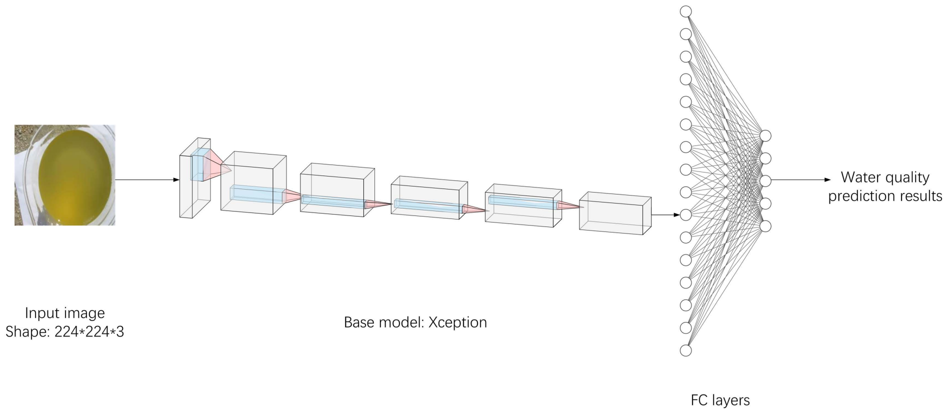


**Fig. 3** *The main structure of the proposed model.*

The structure of Fig. 3 can be divided into four parts: the input layer, the basic model, the fully connected layer, and the output layer. First, the water quality image is processed by the input layer and enters the transfer learning model. The basic model extracts the features of the image. Fully connected layers make decisions based on the extracted image features. The output layer outputs water quality prediction results.

### 2.3.4 Training process of proposed model

**(1) Forward propagation** After the data is input into the model, the output is obtained through the calculation of the first neural network layer, and the output is used as the input of the next neural network layer. Maintaining forward propagation, passing to the last neural network layer, and is activated by the softmax activation function. The forward propagation is over. In the data representation, each layer of neurons in a fully connected neural network is represented as a column vector. The neurons in each layer will take the output of the neuron in the previous layer as input, multiply it by the weight matrix and add the bias term in the form of a column vector to get the output value before activation. Finally, get the final value of this layer through the activation function. The output after activation, the specific calculation formula is as follows:

$$z^{(l)} = w^{(l)} \times a^{(l-1)} + b^{(l)}, \tag{2}$$

$$a^{(l)} = \sigma^{(l)}(z^{(l)}), \tag{3}$$

where $z^{(l)}$ is the column vector before activation of the neural network at layer $l$, $w^{(l)}$ is the weight matrix from layers $l-1$ to $l$, and $a^{(l-1)}$ is the output value of the neural network in the layer $l-1$, $b^{(l)}$ is the bias vector. $\sigma^{(l)}$ is the activation function of the layer $l$, and $a^{(l)}$ is the output value of the layer $l$.

In our proposed model, the last fully connected layer will output the probability value of each classification through the softmax activation function. Finally, the model will select the category with the highest classification probability as the final decision. The formula for the softmax activation function [7] is as follows:

$$a_i = \frac{e^{z_i}}{\sum\limits_k e^{z_k}}, \tag{4}$$

where $a_i$ represents the $i$-th category probability output by the softmax function, $e$ is the natural index, $z_i$ is the $i$-th input value of softmax, and $k$ represents the set of integers between 0 and the number of categories.

After that, the network model selects the classification with the highest probability among the classification probabilities given by the softmax function as the prediction classification of the network model. In this way, when the column vector $x$ is input to the network model, the output y of our final neural network can be obtained through layer-by-layer calculations. The forward propagation of the neural network is completed.

**(2) Back propagation** The ultimate purpose of the network model is to predict the labels of the input data as accurately as possible. Therefore, a large amount of labeled data needs to be given to the neural network. Not only input data to the network model, but also tell it what the corresponding output is, and let the neural network learn to adjust the internal parameters. The back-propagation algorithm can realize the parameter adjustment of the neural network. Back-propagation can be divided into two steps. First, the error between the actual label and the prediction result is quantified by a loss function. Then the gradient descent method is used to optimize the model weights. The gradient descent method is a method of feeding back the output error to the neural network and automatically adjusting the parameters. It calculates the derivative of the output error's loss value to the neural network weight $\mathbf{W}$ and adjusts $\mathbf{W}$ in the opposite direction of the derivative. Repeat this operation until the loss value is minimized.

The loss function in our proposed model is categorical cross-entropy. It is calculated as follows:

$$L = -\sum_k y_k \cdot \log a_k, \tag{5}$$

where $y_k$ is the actual label of classification $k$. $a_k$ is the predicted probability of classification $k$ output by the softmax function of Eq. (4). The parameter $k$ represents the set of integers between 0 and the number of categories.

Then $L$ calculates the partial derivative of the output $f_i$ of the neuron in the fully connected layer before softmax as follows:

$$\frac{\partial L}{\partial f_i} = \sum_k \frac{\partial L}{\partial a_k} \cdot \frac{\partial a_k}{\partial f_i}, \tag{6}$$

where $L$ is the cross-entropy loss function. $f_i$ is the $i$-th neuron output of the fully connected layer before the softmax function, and $a_k$ is the output value of the $k$-th classification activated by the softmax function. $k$ represents the set of integers between 0 and the number of categories.

The partial derivatives of the weights are calculated iteratively to obtain the errors of the parameters, and then the gradient descent algorithm is used to optimize and update the weights.

$$w_{i,j}^{(l)} = w_{i,j}^{(l)} - \alpha \cdot \frac{\partial L(w)}{\partial w_{i,j}^{(l)}}, \tag{7}$$

where $w_{i,j}^{(l)}$ represents the weight of the $i$-th neuron in the $l-1$ layer to the $j$-th neuron in the layer $l$, $\alpha$ is the learning rate, and $L(w)$ is the loss function.

After the weight optimization is completed, the back-propagation algorithm ends. After all the training data has passed forward and backward propagation, the model training is completed.

# 3. Results and discussion

## 3.1 Experimental setups

The experiments were performed on an Nvidia Tesla M10-based server. The Nvidia Tesla M10 integrates four GPU cores on one graphics card, and these four GPUs use the Maxwell architecture. Besides, Nvidia Tesla M10 has 32 GB GDDR5 video memory. The total number of CUDA cores for the NVIDIA Tesla M10 is 2560 (640 per GPU).

The server uses the following environment configuration: Linux, Python3.6, TensorFlow as the backend, and Keras as the front-end. Xshell and Xftp6 are used on the server to complete server access and file access.

Tab. II shows the default settings of the hyperparameters in the experiment. Unless otherwise specified, hyperparameters in experiments are default values. RMSprop was selected as the optimizer during training, where the initial learning rate is 0.001, the decay rate of the moving average of RMSprop gradient squarer is 0.9, epsilon is set to None, decay parameter is set to 0.7. The ratio of the training set to the test set is 8:2. In addition, to prevent the model from overfitting, the model uses Keras built-in image augmentation technology, including image rotation, image cropping, graying, image translation, and image affine transformation. The relevant code will be uploaded to the website after code review: `https://github.com/Xingcun-Li/Water-color-classification`.

| Hyperparameter name | Parameter setting |
|---|---|
| Batch size | 32 |
| Epoch | 30 |
| Initial learning rate | 0.001 |
| Rho | 0.9 |
| Epsilon | None |
| Decay | 0.7 |
| Train test split | 0.8 |

**Tab. II** *Default settings of hyperparameters in experiments.*

## 3.2 Performance evaluation

In this section, image classification evaluation metrics are used to evaluate the performance of our proposed model.

### 3.2.1 Accuracy and loss

The experimental hyperparameters adopt default parameters and configurations. First, a divided training set is used to input to the proposed model. Next, the test set is used to evaluate the trained model. The evaluation results are shown in Fig. 4 and Fig. 5.

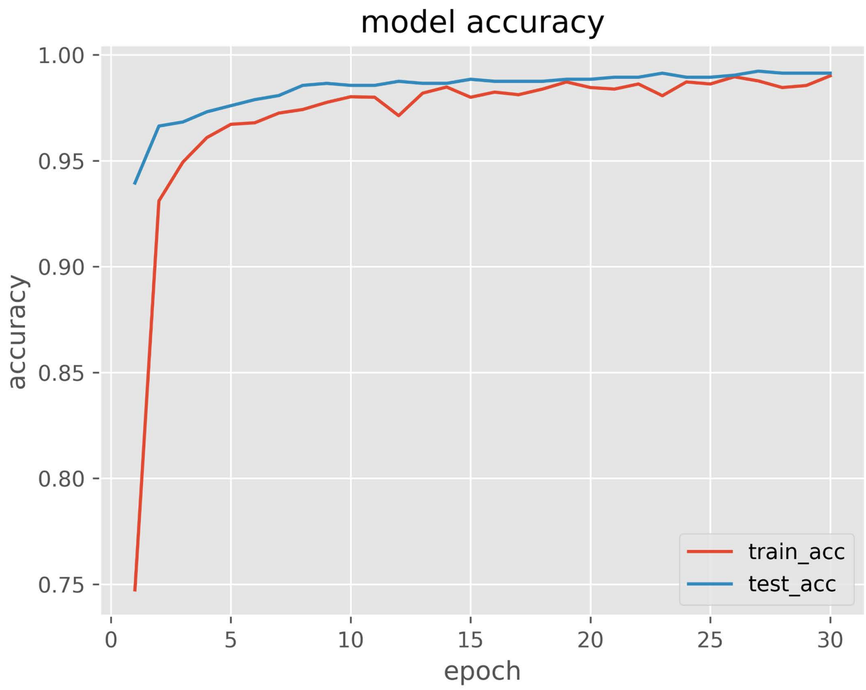


**Fig. 4** *Evaluation of the accuracy of our proposed model.*

Figs. 4 and 5 respectively plot the accuracy and loss of our proposed model as a function of the epoch. The accuracy of the model is divided into a training set curve and a test set curve. The accuracy increases rapidly with the increase of epoch, and the loss function decreases sharply, which means that the model has improved performance in the process of continuous learning. When the epoch reaches the final condition, the accuracy of the training set is 0.9868, and the loss is 0.0434, while the accuracy of the test set is 0.9914, and the loss is 0.0375, and the model performs well.

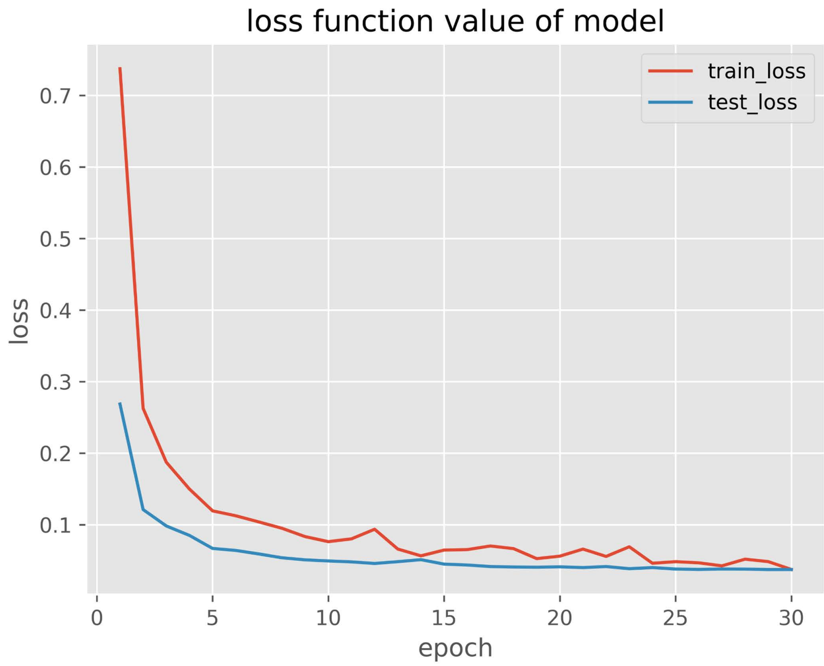


**Fig. 5** *Evaluation of the loss function value of our proposed model.*

### 3.2.2 Confusion matrix

Confusion matrix, also called the error matrix, is a standard format for expressing accuracy evaluation, and it is expressed in a matrix form with n rows and n columns. In image accuracy evaluation, it is mainly used to compare the classification result with the actual measured value. The accuracy of the classification result can be displayed in a confusion matrix. Each column of the confusion matrix represents the prediction category, and the total of each column represents the number of data predicted for that category. Each row represents the correct category of the data, and the total amount of data in each row represents the number of data instances in that category. The scikit-learn toolbox and the model developed by Keras are used to obtain the confusion matrix for the proposed method.

From the confusion matrix in Tab. III, it can be observed that the model has the best classification effect for label 3. The model correctly classified all images with label 3, and there was no misclassification of images with other labels as 3. The model is also useful for the classification of 4 labels, but there is a slight error in the classification of images of other labels.

## 3.3 Precision, recall and F1-score

For the binary classification problem, there are three commonly used evaluation metrics: precision, recall, and F1-score. First, get the confusion matrix for binary classification, as shown in Tab. IV.

| Label | Predict 0 | Predict 1 | Predict 2 | Predict 3 | Predict 4 |
|---|---|---|---|---|---|
| 0 | 194 | 0 | 2 | 0 | 0 |
| 1 | 0 | 211 | 0 | 0 | 2 |
| 2 | 3 | 2 | 220 | 0 | 0 |
| 3 | 0 | 0 | 0 | 202 | 0 |
| 4 | 0 | 0 | 0 | 0 | 205 |

**Tab. III** *Confusion matrix for our proposed method.*

| Label | Predict 1 | Predict 0 |
|---|---|---|
| 1 | TP | FN |
| 0 | FP | TN |

**Tab. IV** *Confusion matrix for binary classification.*

The first letter in TP, TN, FP, and FN is to judge whether the prediction result is correct based on the actual label (True: T, False: F). The second letter in TP, TN, FP, FN is the prediction result of the deep learning model (positive: P, negative: N)

Based on these theories, precision and recall and F1-score can be calculated by the following formula:

$$precision = \frac{TP}{TP + FP}, \tag{8}$$

$$recall = \frac{TP}{TP + FN}, \tag{9}$$

$$F1\text{-}score = \frac{2PR}{P + R}, \tag{10}$$

where $P$ and $R$ are abbreviations for precision and recall.

These performance metrics cannot be directly used for image multi-classification problems. A common approach is to convert the multi-classification problem of images into a two-classification problem using these evaluation parameters. For example, the third category of water color is taken as true and the other categories as false. The model predicts that the third category is a positive example, and the other categories are negative. Therefore, each category can calculate the corresponding precision and recall and F1-score. The experimental calculation results are shown in Tab. V.

In Tab. V, the performance metrics of each label are presented. The macro-averaging method evaluates the overall metrics of the model.

| Label | Precision | Recall | F1-score | Number of samples |
|---|---|---|---|---|
| 0 | 0.98 | 0.99 | 0.99 | 196 |
| 1 | 0.99 | 0.99 | 0.99 | 213 |
| 2 | 0.99 | 0.98 | 0.98 | 225 |
| 3 | 1.00 | 1.00 | 1.00 | 202 |
| 4 | 0.99 | 1.00 | 1.00 | 205 |
| Macro avg | 0.99 | 0.99 | 0.99 | 1041 |

**Tab. V** *Precision, recall and F1-score of the proposed model.*

### 3.4 Comparison experiments with other deep learning algorithms

The proposed models are compared with other deep learning models in the experiments. Referring to Fig. 1, the comparison group includes four pre-trained models, VGG19, ResNet50, DenseNet121, and InceptionV3.

The accuracy of the proposed model and the comparison group models are shown in Tab. VI, and the proposed model achieved the highest accuracy. In the comparison group, VGG19 achieved the lowest accuracy of 0.97. ResNet50 demonstrated promising generalization capabilities, achieving an accuracy of 0.983. DenseNet121 and InceptionV3 achieved similar performance. The accuracy of the proposed model is better than the comparison group, achieving an accuracy of 0.991.

| Model | Accuracy |
|---|---|
| VGG19 | 0.970 |
| ResNet50 | 0.983 |
| DenseNet121 | 0.981 |
| InceptionV3 | 0.979 |
| Proposed model | **0.991** |

**Tab. VI** *Accuracy on the test set by the proposed model and the comparison group.*

### 3.5 Discussion

A server environment was built to implement the proposed model to learn water color classification knowledge from the dataset, and hyperparameters were set in the experiments. The training process of the model was done on the server, and the accuracy and loss curves of the model with epoch were plotted. The commonly used multi-class metrics were used to evaluate the performance of the model. The experimental results and evaluation results show that the accuracy of the test set of the model is 0.9914, the loss is 0.0434, and the macro precision and macro recall of the model calculated by the macro averaging method of the model and the macro

F1-score are both 0.99. Based on the above parameters, the performance of the model is excellent.

# 4. Conclusions

In fisheries aquaculture, the quality of aquaculture water is a matter of concern. If water quality is not managed correctly, it will be difficult for aquaculture organisms to survive, which will have a considerable impact on the economic benefits of aquaculture personnel. In aquaculture scenarios, the water color is often used as an important method for identifying water quality by experienced aquaculture personnel. However, since this observation method can usually only be done by experienced aquaculture experts, it is difficult to promote. The purpose of this paper is to complete the water quality analysis based on water color with a digital and scalable solution. 5203 water quality images from real environments were collected to form a water quality image dataset. Based on the dataset, an artificial intelligence-based deep transfer learning strategy is proposed to automatically complete water quality classification from the labeled high-quality water quality image dataset. The design ideas and architecture of the transfer learning model and the training steps of the neural network layer are explained. Finally, the proposed model is tested by the performance metrics of image multi-classification. Experimental results show that our proposed model has excellent performance.

# References


[1] BOSMA R., ANH P.T., POTTING J. Life cycle assessment of intensive striped catfish farming in the Mekong Delta for screening hotspots as input to environmental policy and research agenda. The International Journal of Life Cycle Assessment. 2011, 16, 903.

[2] BOYD C.E., TUCKER C.S. Handbook for aquaculture water quality. Handbook for Aquaculture Water Quality, 2014, 439.

[3] BOYD C.E., QUEIROZ J., LEE J., ROWAN M., GROSS A. Environmental Assessment of Channel Catfish Ictalurus punctatus Farming in Alabama. Journal of the World Aquaculture Society. 2000, 31, pp. 511–544.

[4] BROOKS B.W., CONKLE J.L. Commentary: Perspectives on aquaculture, urbanization and water quality. Comp Biochem Physiol C Toxicol Pharmacol. 2019, 217, pp. 1–4.

[5] CHOLLET F. Xception: Deep learning with depthwise separable convolutions, Proceedings of the IEEE conference on computer vision and pattern recognition, 2017, pp. 1251–1258.

[6] CHUNTAPA B., POWTONGSOOK S., MENASVETA P. Water quality control using Spirulina platensis in shrimp culture tanks. Aquaculture. 2003, 220, pp. 355–366.

[7] DUNNE R.A., CAMPBELL N.A. On the pairing of the softmax activation and cross-entropy penalty functions and the derivation of the softmax activation function, Proc. 8th Aust. Conf. on the Neural Networks, Melbourne. Citeseer, 1997, pp. 185.

[8] FANG G., ZENG F., LI X., YAO L. Word2vec based deep learning network for DNA N4-methylcytosine sites identification. Procedia Computer Science, 2021, 187, pp. 270–277.

[9] FIGUEIRÓ C.S.M., BASTOS DE OLIVEIRA D., RUSSO M.R., CAIRES A.R.L., ROJAS S.S. FISH farming water quality monitored by optical analysis: The potential application of UV–Vis absorption and fluorescence spectroscopy. Aquaculture. 2018, 490, pp. 91–97.

[10] FURLEY T.H., BRODEUR J., SILVA DE ASSIS H.C., CARRIQUIRIBORDE P., CHAGAS K.R., CORRALES J., DENADAI M., FUCHS J., MASCARENHAS R., MIGLIORANZA

K.S. Toward sustainable environmental quality: Identifying priority research questions for Latin America. Integrated environmental assessment and management. 2018, 14, pp. 344–357.

[11] GOLDBURG R., TRIPLETT T. Murky Waters: Environmental Effects of Aquaculture in the United States, 1997.

[12] GONZÁLEZ-MÁRQUEZ L.C., TORRES-BEJARANO F.M., TORREGROZA-ESPINOSA A.C., HANSEN-RODRÍGUEZ I.R., RODRÍGUEZ-GALLEGOS H.B. Use of LANDSAT 8 images for depth and water quality assessment of El Guájaro reservoir, Colombia. Journal of South American Earth Sciences. 2018, 82, pp. 231–238.

[13] HIRSCH R.M., ALEXANDER R.B., SMITH R.A. Selection of methods for the detection and estimation of trends in water quality. Water resources research. 1991, 27, pp. 803–813.

[14] HONGPIN L., GUANGLIN L., WEIFENG P., JIE S., QIUWEI B. Real-time remote monitoring system for aquaculture water quality. International Journal of Agricultural and Biological Engineering. 2015, 8, pp. 136–143.

[15] LECUN Y., BENGIO Y., HINTON G. Deep learning. Nature. 2015, 521, pp. 436–444.

[16] LI Y., WANG X., ZHAO Z., HAN S., LIU Z. Lagoon water quality monitoring based on digital image analysis and machine learning estimators. Water Research. 2020, 172, 115471.

[17] LIN C.K., SHRESTHA M.K., YI Y., DIANA J.S. Management to minimize the environmental impacts of pond effluent: harvest draining techniques and effluent quality. Aquacultural Engineering. 2001, 25, pp. 125–135.

[18] MAILLARD V.M., BOARDMAN G.D., NYLAND J.E., KUHN D.D. Water quality and sludge characterization at raceway-system trout farms. Aquacultural Engineering. 2005, 33, pp. 271–284.

[19] MANHONG L., HONGXIAN Y., QIGEN L. Water quality evaluation index system of freshwater aquaculture pond. Agricultural Science and Technology, 2011.

[20] MOHANTY R.K., AMBAST S.K., PANIGRAHI P., MANDAL K.G. Water quality suitability and water use indices: Useful management tools in coastal aquaculture of Litopenaeus vannamei. Aquaculture. 2018, 485, pp. 210–219.

[21] MORGAN B.J., STOCKER M.D., VALDES-ABELLAN J., KIM M.S., PACHEPSKY Y. Drone-based imaging to assess the microbial water quality in an irrigation pond: A pilot study. Science of The Total Environment, 2019, 135757.

[22] NI M., YUAN J.-L., LIU M., GU Z.-M. Assessment of water quality and phytoplankton community of Limpenaeus vannamei pond in intertidal zone of Hangzhou Bay, China. Aquaculture Reports. 2018, 11, pp. 53–58.

[23] PAN S.J., YANG Q. A Survey on Transfer Learning. IEEE Transactions on Knowledge & Data Engineering. 2010, 22, pp. 1345–1359.

[24] SAADI A.M.E., YOUSRY M.M., JAHIN H.S. Statistical estimation of Rosetta branch water quality using multi-spectral data.

[25] SCHWARTZ M.F., BOYD C.E. Channel catfish pond effluents. The Progressive Fish-Culturist. 1994, 56, pp. 273–281.

[26] SEOK K., LEONARD S., BOYD C.E., SCHWARTZ M.E. Communications: Water Quality in Annually Drained and Undrained Channel Catfish Ponds over a Three-Year Period. The Progressive Fish-Culturist. 1995, 57, pp. 52–58.

[27] SIMBEYE D.S., YANG S.F. Water quality monitoring and control for aquaculture based on wireless sensor networks. Journal of networks. 2014, 9, p. 840.

[28] TUCKER C.S., HARGREAVES J.A. Environmental Best Management Practices for Aquaculture, 2009.

[29] VAN DEN BRINK P.J., BOXALL A.B.A., MALTBY L. Toward sustainable environmental quality: Priority research questions for Europe. Environ Toxicol Chem. 2018, 37, pp. 2281–2295.

[30] WANG X., MA T. Application of remote sensing techniques in monitoring and assessing the water quality of Taihu Lake. Bulletin of environmental contamination and toxicology. 2001, 67, pp. 863–870.

[31] WEIQI H.E., LIU X., CHEN J., CHEN S. Water quality monitoring in a slightly-pollutedinland water body through remote sensing - Case study of the GuantingReservoir in Beijing, China. Frontiers of Environmental Science & Engineering in China. 2008, 2.

[32] ZENG F., LI X., DENG X., YAO L., LIAN G. An image classification model based on transfer learning for ulcerative proctitis. Multimedia Systems, 2021, 27(4), pp. 627–636.